SMC-TR-99-22

AEROSPACE
REPORT NO.
TR-99(1413)-5

Free-Falling SRMU Segment Impact Orientation Analysis

June 1999

Prepared by

D. M. Moody and K. R. Bohman
Vehicle Systems Division
Engineering and Technology Group

Prepared for

SPACE AND MISSILE SYSTEMS CENTER
AIR FORCE MATERIEL COMMAND
Los Angeles Air Force Base, CA 90245

Contract No. F04701-93-C-0094

National Systems Group

THE AEROSPACE CORPORATION
El Segundo, California

This report was submitted by The Aerospace Corporation, El Segundo, CA 90245-4691, under Contract No. F04701-93-C-0094 with the Space and Missile Systems Center, P.O. Box 92960, Los Angeles AFB, CA 90009-2960. It was reviewed and approved for The Aerospace Corporation by C. S. Gran, Principal Director, Vehicle Systems Subdivision. Captain William Kempf was the project officer.

This report has been reviewed by the Public Affairs Office (PAS) and is releasable to the National Technical Information Service (NTIS). At NTIS, it will be available to the general public, including foreign nationals.

This technical report has been reviewed and is approved for publication. Publication of this report does not constitute Air Force approval of the report's findings or conclusions. It is published only for the exchange and stimulation of ideas.

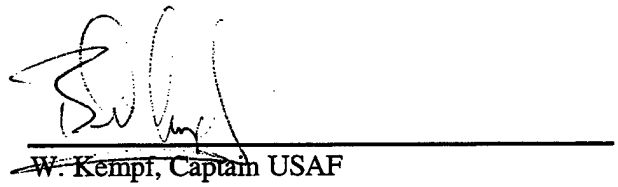

W. Kempf, Captain USAF
Project Officer

REPORT DOCUMENTATION PAGE

Form Approved
OMB No. 0704-0188

1. AGENCY USE ONLY (Leave blank)	2. REPORT DATE	3. REPORT TYPE AND DATES COVERED
	June 1999	

4. TITLE AND SUBTITLE
Free-Falling SRMU Segment Impact Orientation Analysis

5. FUNDING NUMBERS
F04701-93-C-0094

6. AUTHOR(S)
D. M. Moody and K. R. Bohman

7. PERFORMING ORGANIZATION NAME(S) AND ADDRESS(ES)
The Aerospace Corporation
2350 E. El Segundo Blvd.
El Segundo, CA 90245-4691

8. PERFORMING ORGANIZATION REPORT NUMBER
TR-99(1413)-5

9. SPONSORING/MONITORING AGENCY NAME(S) AND ADDRESS(ES)
Space and Missile Systems Center
Air Force Materiel Command
2350 E. El Segundo Blvd.
Los Angeles Air Force Base, CA 90245

10. SPONSORING/MONITORING AGENCY REPORT NUMBER
SMC-TR-99-22

11. SUPPLEMENTARY NOTES

12a. DISTRIBUTION/AVAILABILITY STATEMENT
Public release; distribution unlimited.

12b. DISTRIBUTION CODE

13. ABSTRACT (Maximum 200 words)

A potential consequence of a Titan IV failure early in flight is the ground impact of a Solid Rocket Motor Upgrade (SRMU) segment. Under certain meteorological conditions, the explosion of propellant which results from impact may generate high overpressures (enough to shatter windows) many miles away from the blast source. Human casualties resulting from window breakage following a Titan IV launch failure have become a range safety concern for Vandenberg Air Force Base and surrounding communities over the last few years. ACTA, Inc., the range safety contractor for Vandenberg, has developed a methodology for computing casualty expectation level as a function of launch date and time of day. The ACTA computer code, called BLASTC, currently assumes that all SRMU segment impacts are side-on; which is a worst case, since this orientation gives the highest yield, all other factors being constant. The purposes of this work are (1) to provide a probability distribution of segment impact orientation angles, and (2) to formulate a method by which a given impact angle can be associated with a yield value. These two pieces of information will allow the removal of a current source of unnecessary conservatism in the BLASTC model.

14. SUBJECT TERMS
blast, casualties, overpressure, range safety, solid rocket propellant, Titan IV

15. NUMBER OF PAGES
23

16. PRICE CODE

17. SECURITY CLASSIFICATION OF REPORT	18. SECURITY CLASSIFICATION OF THIS PAGE	19. SECURITY CLASSIFICATION OF ABSTRACT	20. LIMITATION OF ABSTRACT
Unclassified	Unclassified	Unclassified	Unlimited

CONTENTS

1. Introduction

A potential consequence of a Titan IV failure early in flight is the ground impact of a Solid Rocket Motor Upgrade (SRMU) segment. Under certain meteorological conditions, the explosion of propellant which results from impact may generate high overpressures (enough to shatter windows) many miles away from the blast source. BLASTC (Ref. 1) is a tool developed by ACTA Inc. for predicting window breakage and casualties resulting from such launch failure overpressures at Vandenberg Air Force Base.

The yield histogram input to BLASTC currently assumes that all SRMU segment impacts are side-on. The rationale behind this assumption is as follows. Hydro-code calculations of yield, generated for perfectly side-on and perfectly end-on impacts at the same velocity, show that the side-on case gives significantly higher yield (Ref. 2.) There are no code results (nor test data) at intermediate impact angles. Furthermore, it had been previously suggested to ACTA by another agency that free-falling cylindrical bodies would tend to aerodynamically trim to side-on orientation prior to impact. Thus, lacking further information, ACTA adopted the logically conservative approach of assuming side-on impacts in all cases.

Since the assumption of side-on impact for all failures may be a source of undue conservatism, the following two tasks were undertaken by the Aerospace Flight Mechanics Department.

1. Calculation of a probability distribution of impact orientation angles using Monte Carlo techniques to randomly sample initial conditions at some randomly selected time of failure. For given initial conditions, the free-falling six degree-of-freedom trajectory is simulated to the ground, using realistic aerodynamic forces and moments on the SRMU segments. The impact angle in each case is recorded.

2. Formulation of a method by which a given impact orientation angle can be associated with a yield value lying in the range between the side-on and end-on values.

2. Probability Distribution of Impact Angles

A Monte Carlo trajectory simulation technique was used for approximating the segment impact orientation distribution. The simulation initiates a nominal Titan IVB-12 three degree-of-freedom (3DOF) performance trajectory. At a selected time of failure, the simulation "jumps" to modeling an SRMU segment in a 6DOF free-fall (non-thrusting) to ground impact. The mass and moments of inertia are calculated based on the elapsed trajectory time. Aerodynamic coefficients of cylindrical segments of various lengths were provided by the Aerospace Fluid Mechanics Department (Ref. 3.) These coefficients are shown as functions of angle-of-attack in Figs. 1 - 12. Discussions with ACTA (Ref. 4) revealed that scenarios which result in an intact segment impact assume a failure (or partial failure) of the Inadvertent Separation Destruct System (ISDS.) Such a condition is associated with an SRMU case rupture on an otherwise nominal flight. This would imply an on-trajectory failure with initial angle-of-attack and angular rates near nominal. Given these factors, the Monte Carlo analysis assumed a uniformly random failure time in the first 60 seconds of flight, and random normal variation of angle-of-attack and pitch/yaw rates about the nominal state. A standard deviation of 5^o was chosen for the angle-of-attack probability distribution. The standard deviation for the pitch and yaw rates were both chosen to be: 30 deg/sec for a *high rate* analysis, 10 deg/sec for a *medium rate* analysis, and 3 deg/sec for a *low rate* analysis. Another consideration is the possibility of two segments still joined together at impact. Thus, cylinder lengths of 16, 33, 48, and 68 ft were each modeled separately. (In all cases, the diameter is 10.5 ft.)

There were therefore a total of twelve cases considered, viz., the high, medium, and low angular rates for each of the four lengths. In each of these cases, the Monte Carlo sample size was 1000. For each element in a sample, the failure time was drawn uniformly from the first 60 seconds of flight. Variations about the nominal trajectory values (at time of failure) of angle-of-attack and rotation rates were realized by drawing from normal distributions having the standard deviations described above.

The Monte Carlo results for the twelve cases are shown in Table 1, along with the corresponding impact orientation probabilities. Impact orientation angle histograms for the high and low rate analyses for the various segment lengths are shown in Figs. 13-20. [Histograms for the medium rate (10 deg/sec) analyses are not shown, but they look much like much like those for the low rate (3 deg/sec).]

Observations

1. From the histograms for the four cases with the higher standard deviations in initial angular velocity (30 deg/sec), it can be seen that the orientation at impact tends to be uniformly distributed. This results from the fact that for higher initial angular velocities, there is insufficient time in the cases considered here for the body to trim due to aerodynamic moments.

2. For lower initial angular rates (σ_{py} of 10 deg/sec and 3 deg/sec), the longer cylinders (two joined segments, either 48 or 68 ft in length) trim to side-on attitude at impact in slight preference to end-on attitude.

3. For lower initial rates, the short segment (16 ft) tends to trim to an end-on impact, while the single segment (33 ft) tends to prefer a nearly end-on impact (70^o to 80^o.)

σ_{py} = one sigma value for initial pitch/yaw body rates (deg/sec) θ = impact orientation angle from horizontal (deg)										
Length (ft)	σ_{py} (deg/sec)	Prob $0 < \theta < 5$	Prob $5 < \theta < 10$	Prob $10 < \theta < 15$	Prob $15 < \theta < 20$	Prob $20 < \theta < 25$	Prob $25 < \theta < 30$	Prob $30 < \theta < 35$	Prob $35 < \theta < 40$	Prob $40 < \theta < 90$
16	30	0.078	0.073	0.075	0.086	0.065	0.047	0.047	0.040	0.489
	10	0.081	0.065	0.063	0.047	0.041	0.040	0.022	0.025	0.616
	3	0.068	0.065	0.041	0.035	0.027	0.012	0.004	0.008	0.740
33	30	0.077	0.062	0.069	0.066	0.077	0.050	0.044	0.063	0.492
	10	0.112	0.099	0.070	0.067	0.043	0.041	0.033	0.031	0.504
	3	0.087	0.088	0.049	0.039	0.046	0.016	0.012	0.008	0.655
48	30	0.079	0.082	0.069	0.065	0.070	0.061	0.065	0.050	0.459
	10	0.105	0.089	0.077	0.072	0.066	0.058	0.055	0.042	0.436
	3	0.116	0.092	0.089	0.045	0.057	0.031	0.017	0.007	0.546
68	30	0.061	0.050	0.063	0.062	0.056	0.054	0.073	0.056	0.525
	10	0.067	0.061	0.061	0.069	0.064	0.067	0.060	0.062	0.489
	3	0.071	0.079	0.076	0.081	0.086	0.087	0.069	0.063	0.388
Uniform Dist.		0.0556	0.0556	0.0556	0.0556	0.0556	0.0556	0.0556	0.0556	0.5556

Table 1: Segment Impact Orientation Probability

3. Association of Impact Angle with Yield Value

As stated previously, there are no code results or test data for the explosive yield resulting from the impact of propellant segments at orientations other than perfectly end-on or perfectly side-on. In what follows, a method is proposed by which a yield value may be assigned to an impact of arbitrary orientation.

Mechanical Rotation Time

Consider a cylindrical propellant segment of length L and diameter D impacting the ground. The impact angle, i.e., the angle between the cylinder axis and the ground plane, is denoted by θ (see Fig. 21.) It is assumed that the point of impact (shown as point O in Fig. 21) instantaneously becomes a center of rotation, i.e., the segment is assumed not to bounce on impact. Let v_1 denote the vertical component of center-of-mass velocity just prior to impact, and let v_2 denote the value of this component just after impact.

Conservation of the vertical component of linear momentum implies

$$\mathcal{J}_L = (v_1 - v_2)m \tag{1}$$

where $\mathcal{J}_L$ is the linear impulse delivered by the ground force during impact and m denotes the mass of the segment.

The angular impulse due to the force from the ground induces a post-impact angular velocity, ω_2, which is assumed here to be very large in comparison to any pre-impact angular velocity. Conservation of angular momentum implies

$$\mathcal{J}_A = I_c\,\omega_2 \tag{2}$$

where $\mathcal{J}_A$ is the angular momentum of the ground force about the center of mass and

$$I_c = \frac{mL^2}{12}\left[1+\frac{3}{4}\left(\frac{D}{L}\right)^2\right] \tag{3}$$

is the moment of inertia of the cylinder about a central diameter.

From the rotational kinematics of the problem,

$$\mathcal{J}_A = l_x\,\mathcal{J}_L \tag{4}$$

and

$$v_2 = l_x\,\omega_2 \tag{5}$$

where

$$l_x = l\,\cos\theta' \tag{6}$$

and, from Fig. 21

$$l = \frac{1}{2}\sqrt{L^2+D^2} \quad \text{and} \quad \theta' = \theta + \tan^{-1}(D/L) \tag{7}$$

Substitution of (1), (4), and (5) into (2) eliminates impulse and gives a single equation for ω_2.

$$\omega_2 = \frac{l_x\, v_1}{I_c/m + l_x^2} \tag{8}$$

Now, the time for the cylinder to rotate into full lateral-tangent contact with the ground is

$$\Delta t_{rot} = \frac{\theta}{\omega_2} \tag{9}$$

Combustion Wave Time Scale

It is now desired to compare the rotation time in (9) to the time taken for a combustion wave, initiated by contact at point O (see Fig. 21), to propagate the axial extent L of the segment.

It is assumed, simplistically, that the combustion wave initiated by ground contact propagates vertically to the top surface, then reflects in accord with Shell's law. This process is repeated each time the wave front reaches the lateral surface of the cylinder. Thus, the axial component of the propagation velocity of the wave, due to multiple internal reflections, is

$$c_s \sin\theta$$

where c_s is the combustion wave speed in the propellant. The combustion time scale is therefore

$$\Delta t_c = \frac{L}{c_s \sin\theta} \tag{10}$$

and side-on impacts may now be defined as those for which

$$\Delta t_{rot} \leq \Delta t_c \tag{11}$$

That is, side-on impacts are defined as those cases in which the cylinder rotates into full lateral-tangent contact with the ground *prior* to the creation of an axial relief wave caused by incident wave reflection from the end of the cylinder most distant from the initiation.

Substitution of (8), (9), and (10) into (11) gives

$$\frac{c_s}{v_1\, L}\,(\theta \sin\theta)\left(\frac{I_c/m}{l_x} + l_x\right) \leq 1 \tag{12}$$

as the condition to be met in order for an impact to be considered side-on.

The deflagration wave speed, c_s, in the propellant may be estimated with the aid of data which appear in Fig. 4 on page 23 of Ref. 2. These data are from the SOPHY test series and were taken on propellant segments which were six feet in diameter. Other data are shown for smaller diameter segments, but the SRMU is 10.5 feet in diameter, which makes the SOPHY data the most pertinent. As stated on page 22 of Ref. 2, the composition of the SOPHY

propellant is similar enough to the SRMU propellant that a single reaction model suffices for both. Averaging the 13 measured deflagration velocities which were taken at propagation distances between 1.5 and 4.0 diameters from the booster charge gives

$$c_s \;=\; 3.17 \text{ km/sec} \;=\; 10,400 \text{ ft/sec}$$

as the average deflagration speed. (By way of comparison, the Chapman-Jouget detonation speed in TNT is 4.2 km/sec.) With c_s so determined, equation (12) is now used to plot the threshold angle, θ_c, below which an impact may be considered to be side-on. (See Figs. 22-25.)

Assignment of Yield to an Arbitrary Impact Orientation

It is now desired to assign a yield value to an impact for which the speed, v_1, and angle, θ, are given. It is assumed that values for the side-on yield, z_{side}, and the end-on yield, z_{end}, are known. The following procedure is proposed. For the segment length and impact velocity at hand, the threshold angle, θ_c, is found from the plots in Figs. 22-25. The yield is then assigned to one of the following three values.

$$z \;=\; \begin{cases} z_{side} & \text{if } \theta \;\leq\; \theta_c \\ z_{end} & \text{if } \theta \;\geq\; 2\,\theta_c \\ (z_{end} \;+\; z_{side})/2 & \text{otherwise} \end{cases}$$

The physical reasons for this assignment are, that in the first case, the segment rotates into full lateral contact with the ground before the axial deflagration can propagate the length of the segment, implying that excitation is dominated by side-on impact. In the second case, the axial deflagration has had the opportunity to propagate the length of the segment at least twice before full side contact is made with the ground. Subsequent excitation by side-on contact is secondary, and the explosion strength will be more directly dictated by ground contact with the end of the cylinder. The third case is the intermediate situation in which a simple average of the end-on and side-on values is used.

4. Summary and Conclusions

Impact orientation angle histograms were generated for SRMU segments of four different lengths, using realistic 6DOF free-fall simulations. For high initial rotation rates, the impact orientation angle was found to be uniformly distributed for all segment lengths. For lower initial rotation rates, longer segments were found to trim to side-on impact in slight preference to end-on. For the shorter segments with lower initial rotation rates, the tendency was found to be toward end-on impact.

A method for computing a threshold angle for side-on impact was formulated. For impacts of 200 ft/sec, this angle was found to be approximately 10^o. For impacts of 1000 ft/sec, it was found to be approximately 23^o. For impact angles lying below the threshold, the yield for the event is taken as the perfectly side-on value. For impact angles greater than twice the threshold value, the yield for the event is taken as the perfectly end-on value. Intermediate cases are assigned the average of the side-on and end-on values.

REFERENCES

1. A. I. Bodner, et al, "Program Description for the BLASTC Computer Model," ACTA, Inc., Report No. 95-314/67-02, September 1995.

2. J. L. Maienschein, J. E. Reaugh, and E. L. Lee, "Propellant Impact Risk Assessment Team Report: PERMS Model to Describe Propellant Energetic Response to Mechanical Stimuli," Lawrence Livermore National Laboratory, Report UCRL-ID-130077.

3. S. H. Chen, Private Communication, March 1999.

4. P. D. Wilde, Private Communication, February 1999.

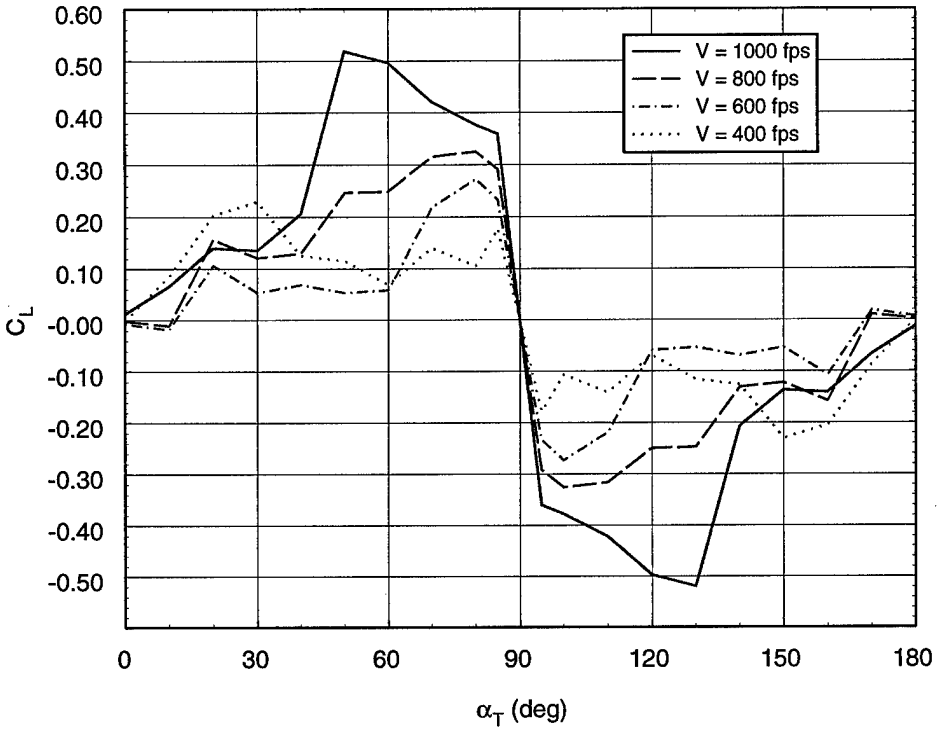

Figure 1: Lift coefficient for 16 ft segment.

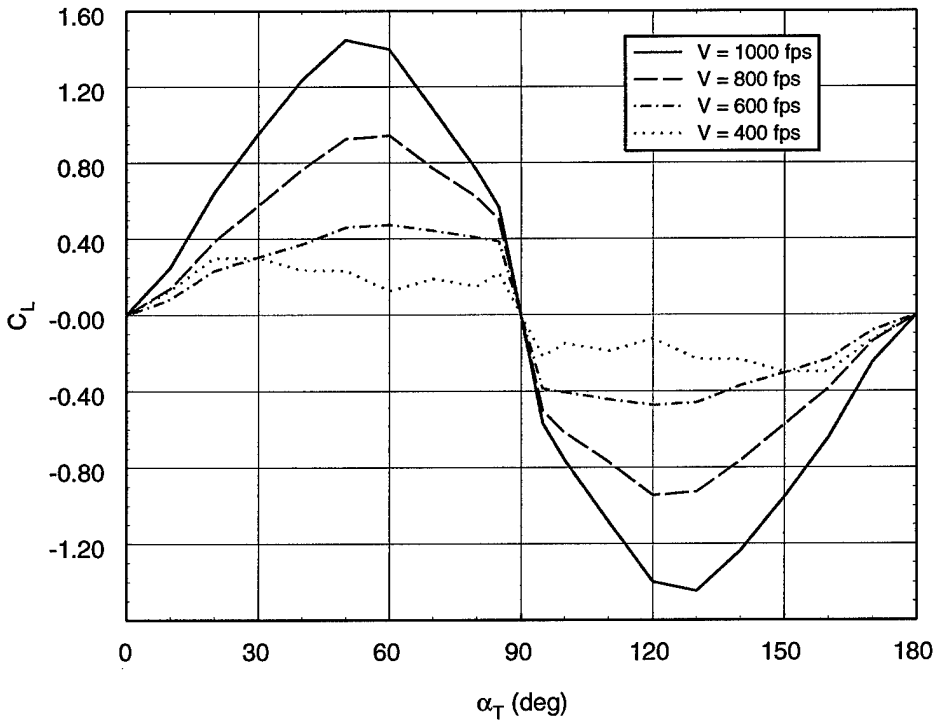

Figure 2: Lift coefficient for 33 ft segment.

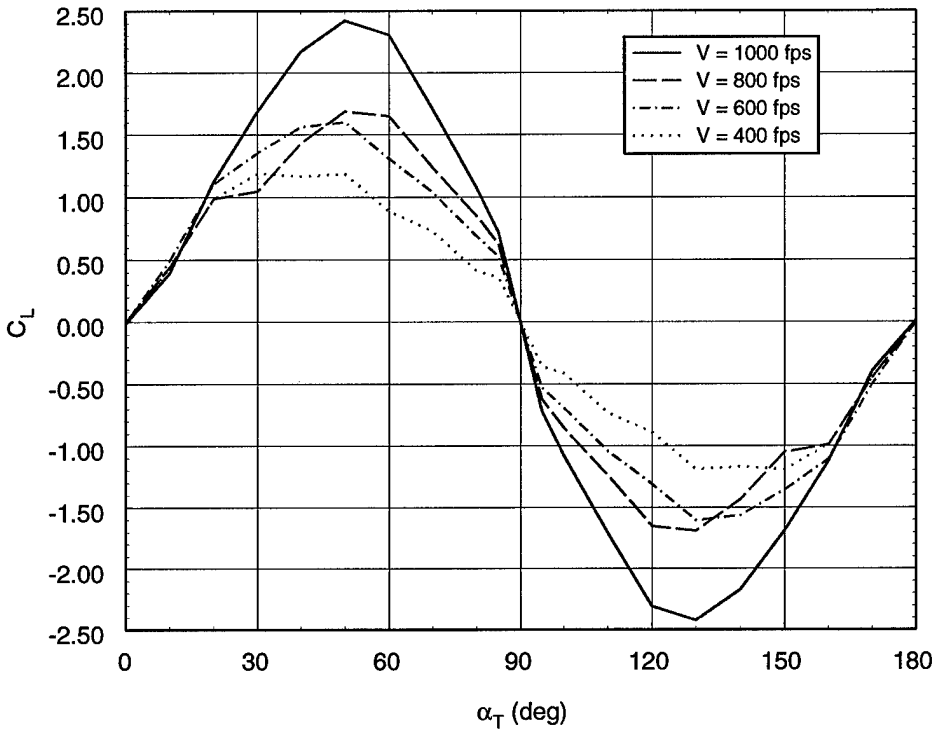

Figure 3: Lift coefficient for 48 ft segment.

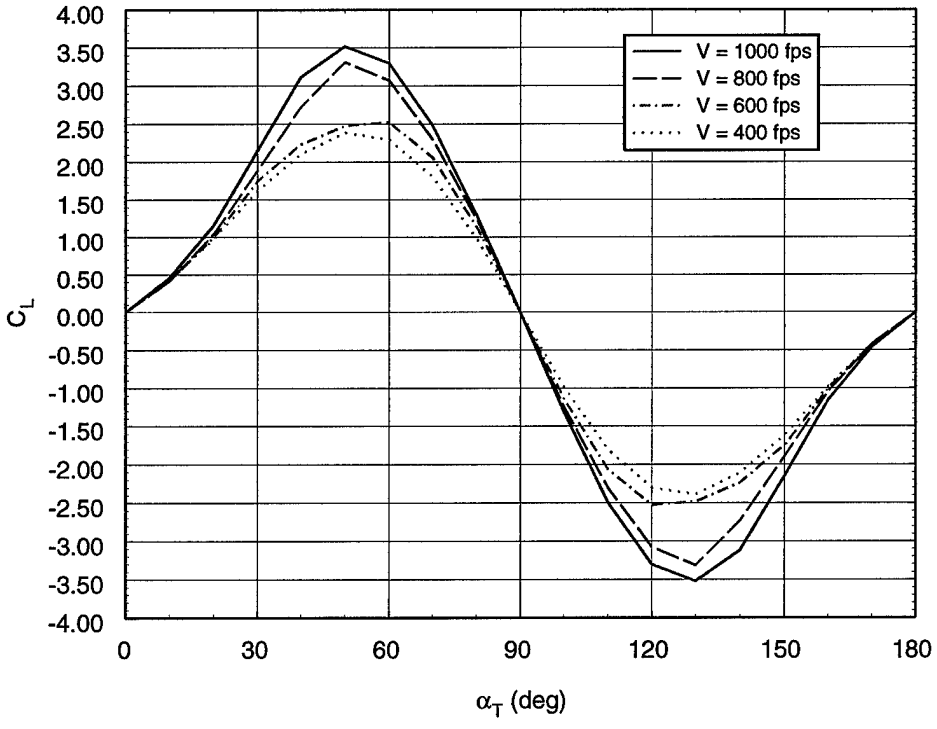

Figure 4: Lift coefficient for 68 ft segment.

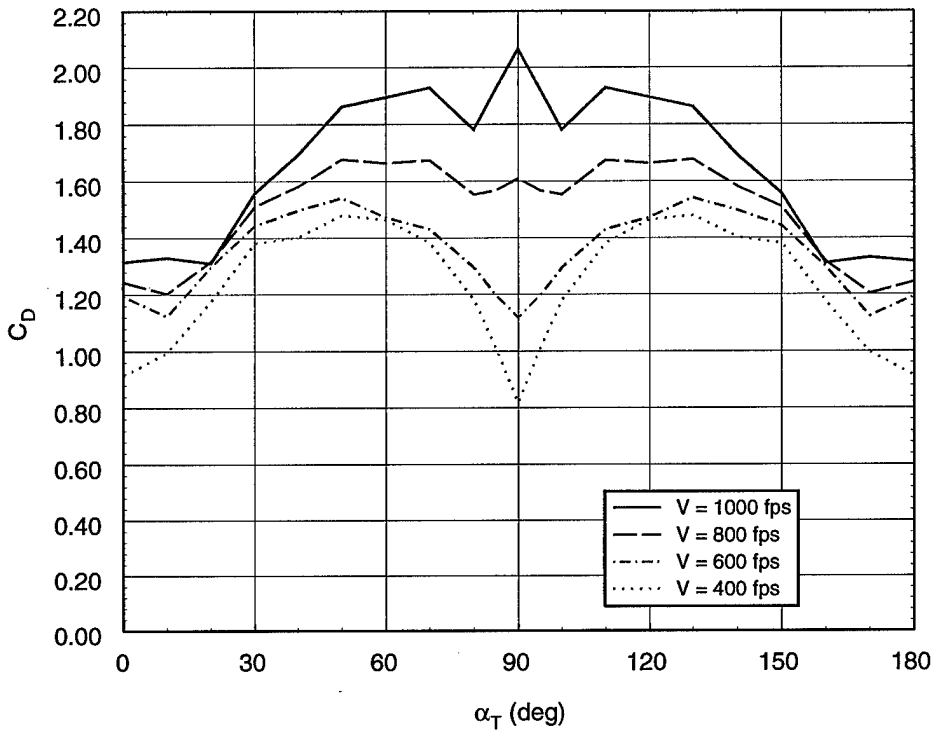

Figure 5: Drag coefficient for 16 ft segment.

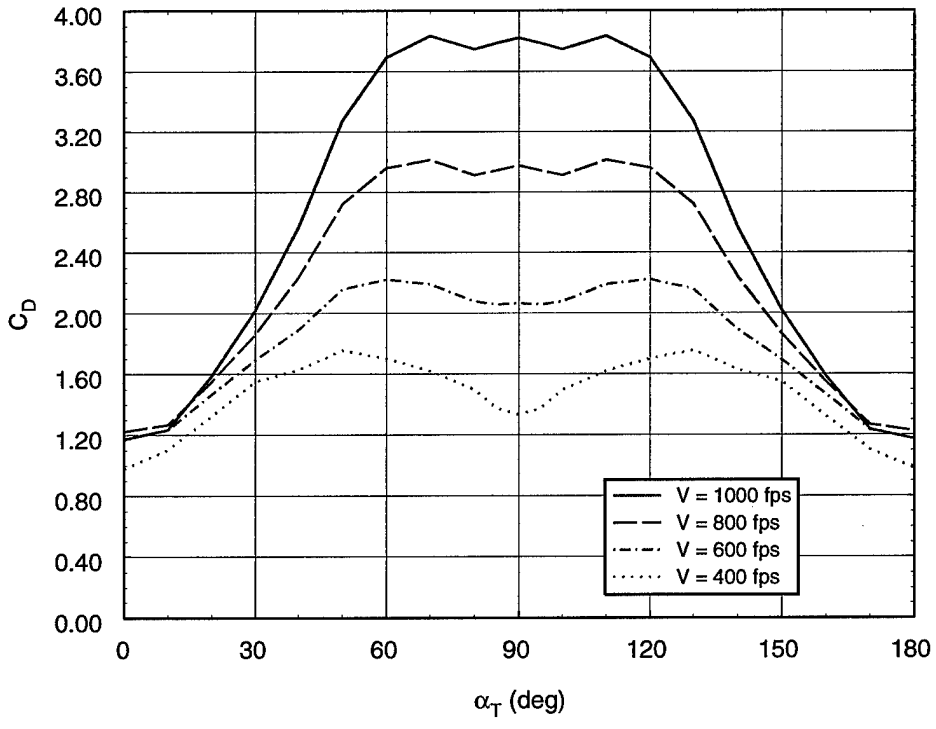

Figure 6: Drag coefficient for 33 ft segment.

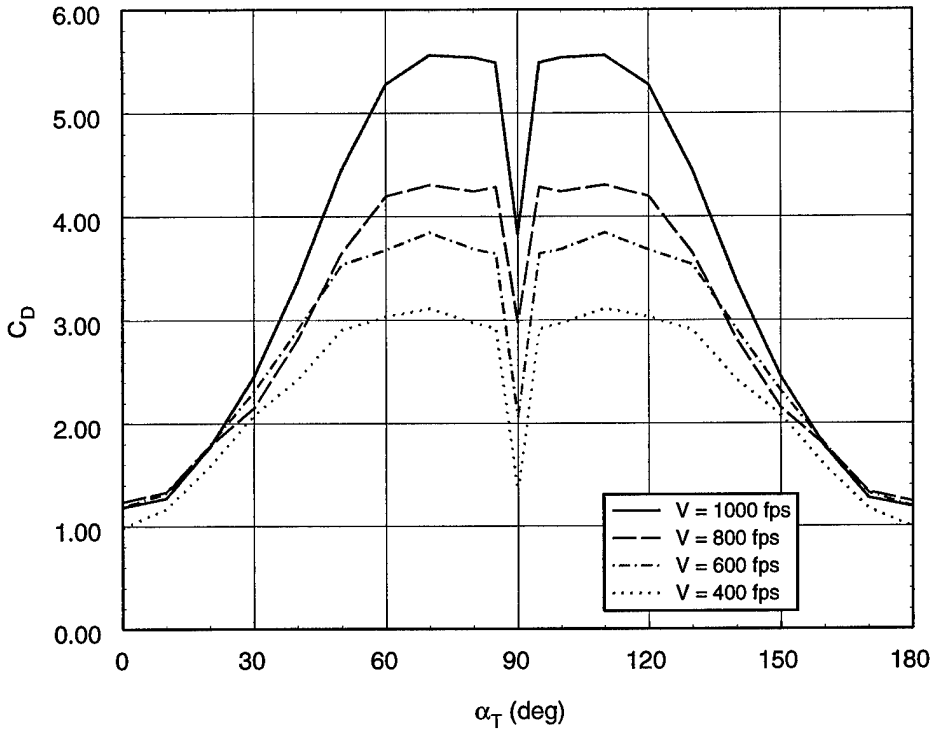

Figure 7: Drag coefficient for 48 ft segment.

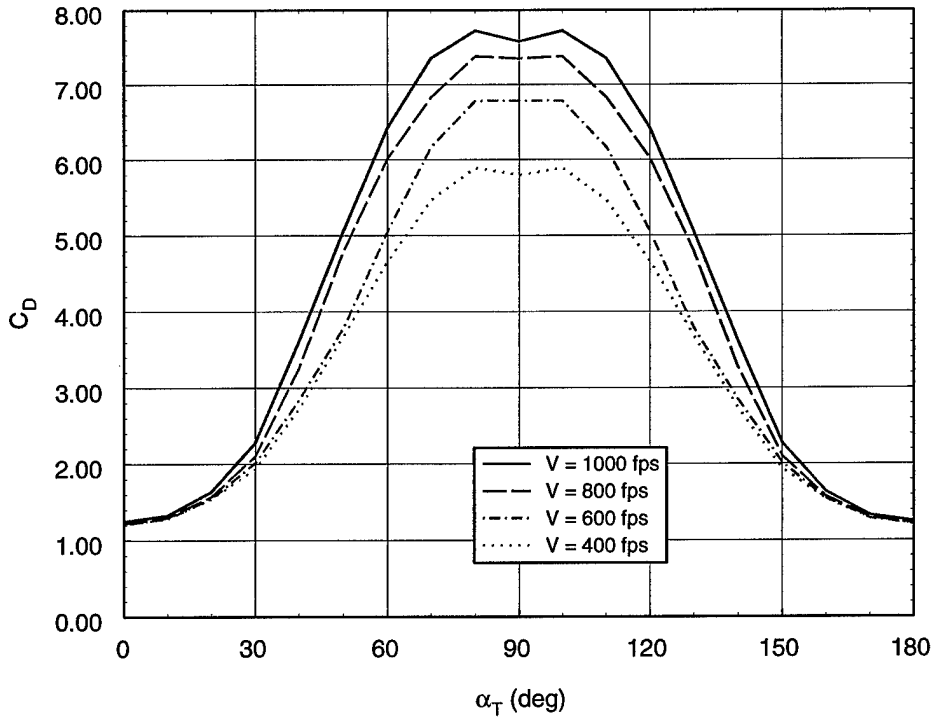

Figure 8: Drag coefficient for 68 ft segment.

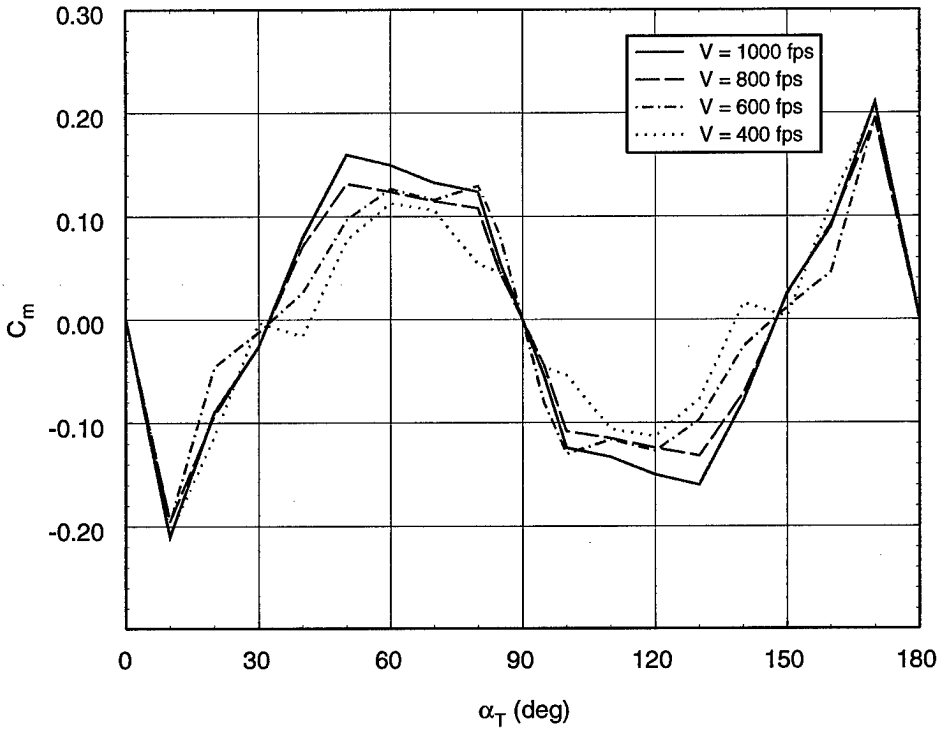

Figure 9: Moment coefficient for 16 ft segment.

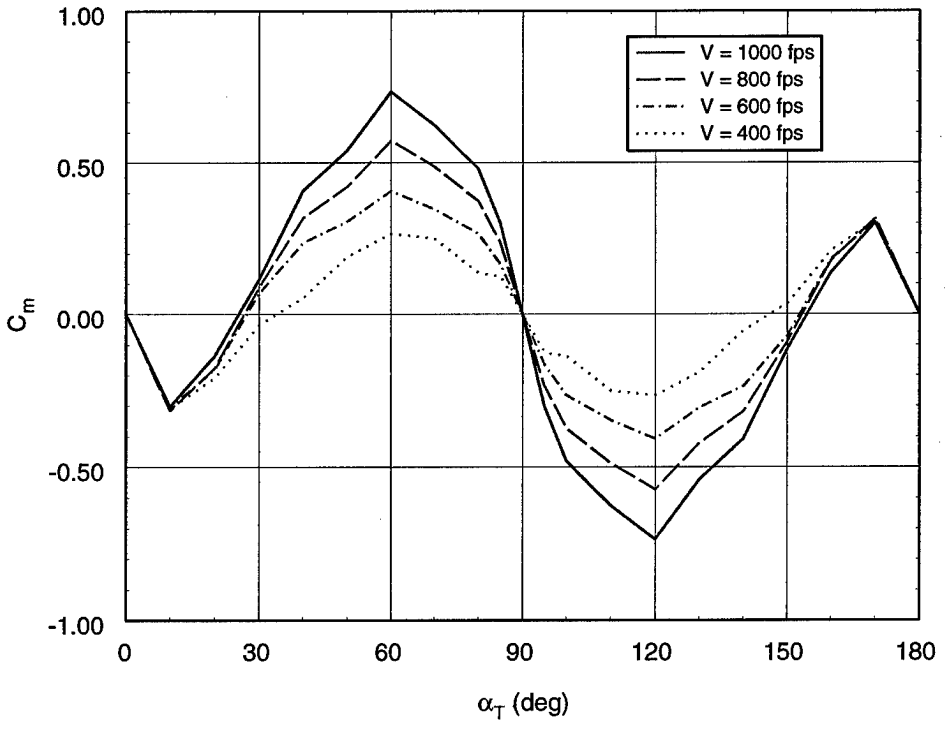

Figure 10: Moment coefficient for 33 ft segment.

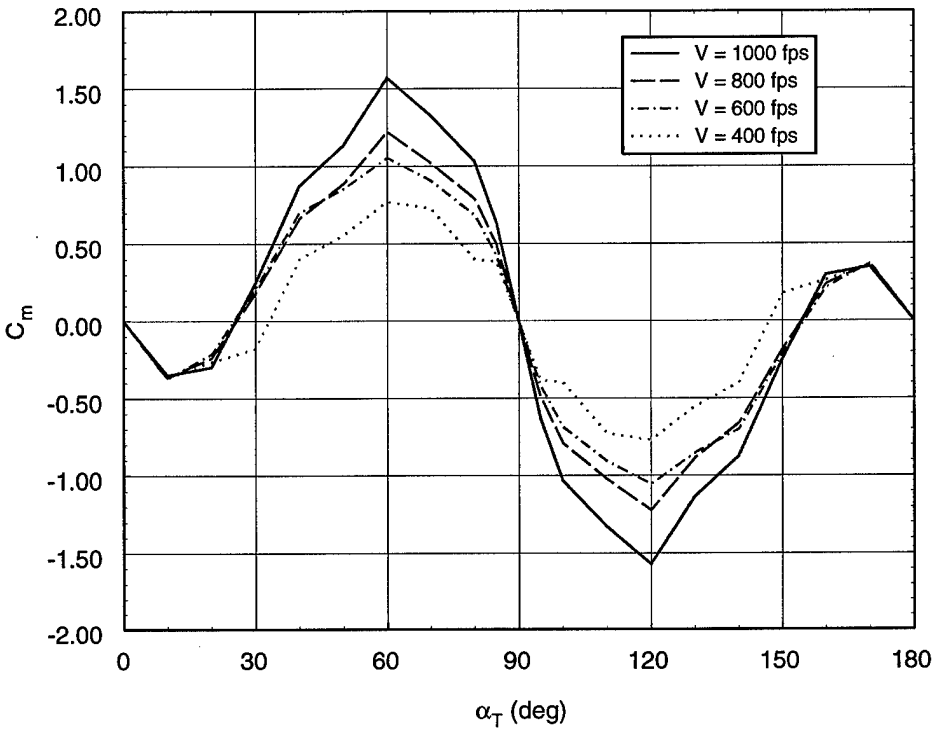

Figure 11: Moment coefficient for 48 ft segment.

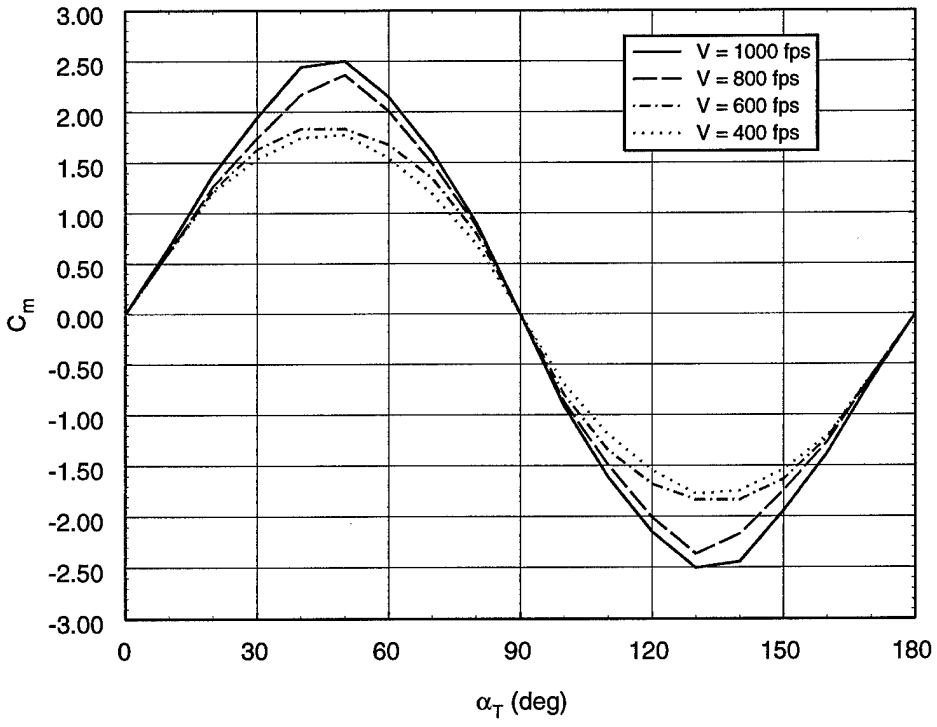

Figure 12: Moment coefficient for 68 ft segment.

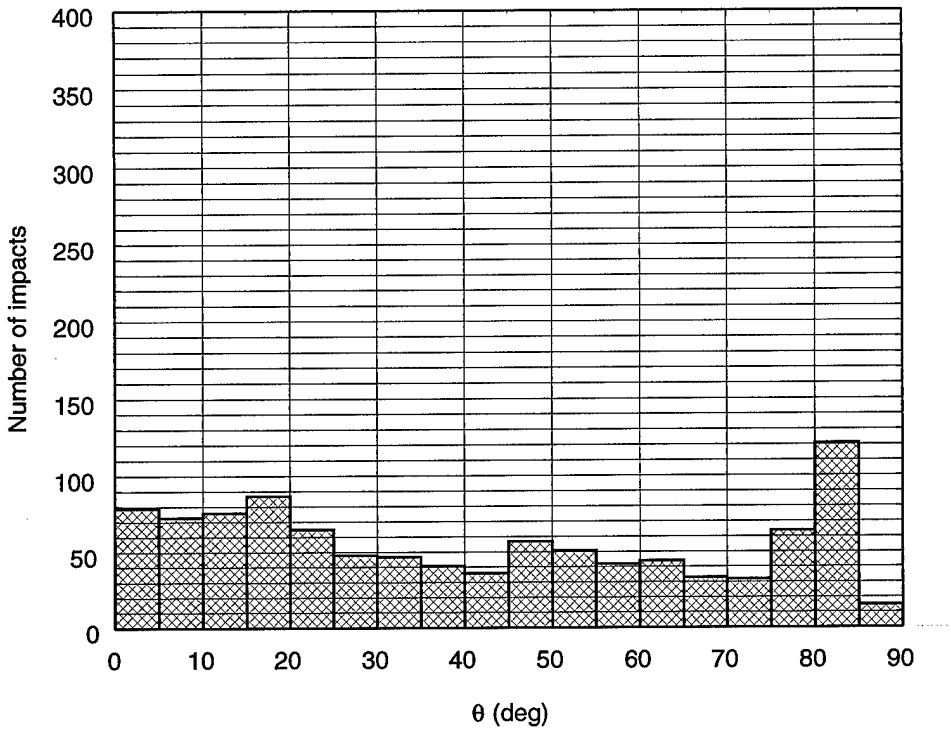

Figure 13: Impact angle histogram for 16 ft segment ($\sigma_{py} = 30$ deg/sec).

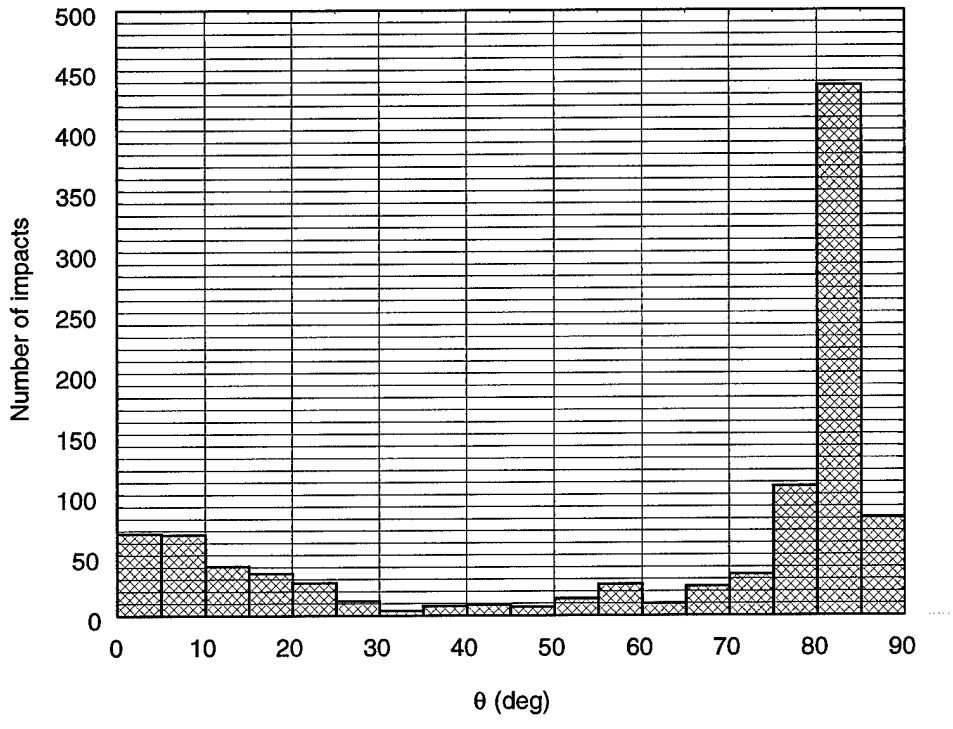

Figure 14: Impact angle histogram for 16 ft segment ($\sigma_{py} = 3$ deg/sec).

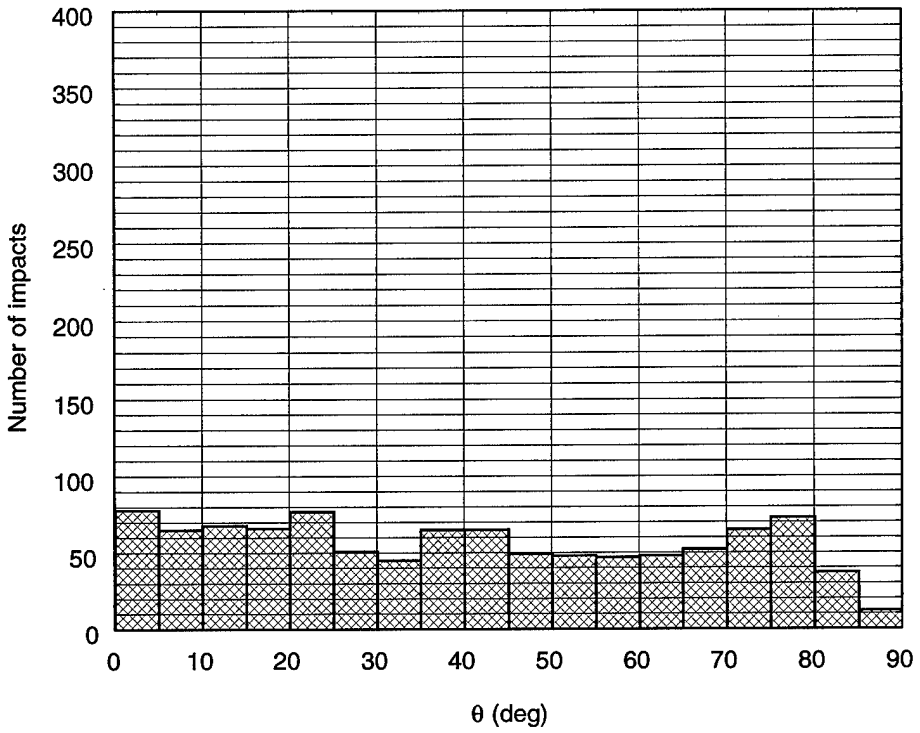

Figure 15: Impact angle histogram for 33 ft segment ($\sigma_{py} = 30$ deg/sec).

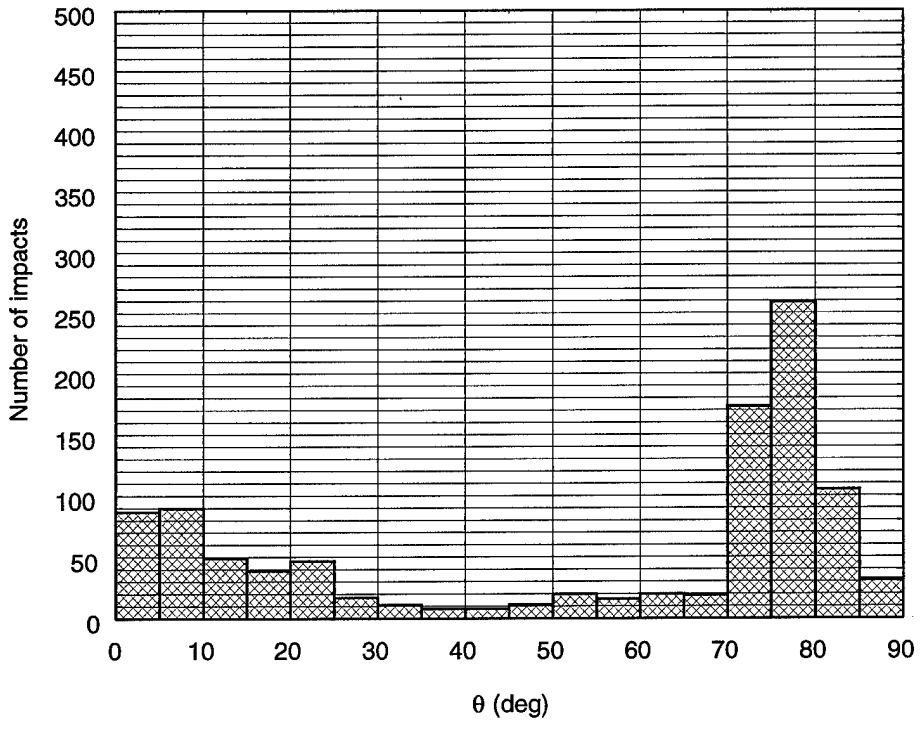

Figure 16: Impact angle histogram for 33 ft segment ($\sigma_{py} = 3$ deg/sec).

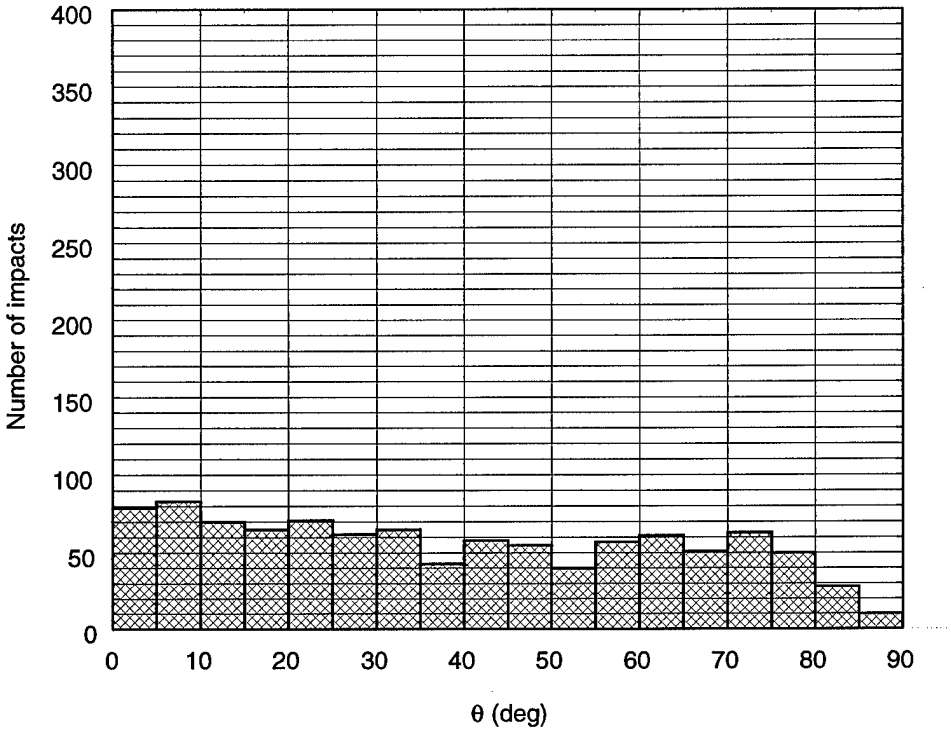

Figure 17: Impact angle histogram for 48 ft segment ($\sigma_{py} = 30$ deg/sec).

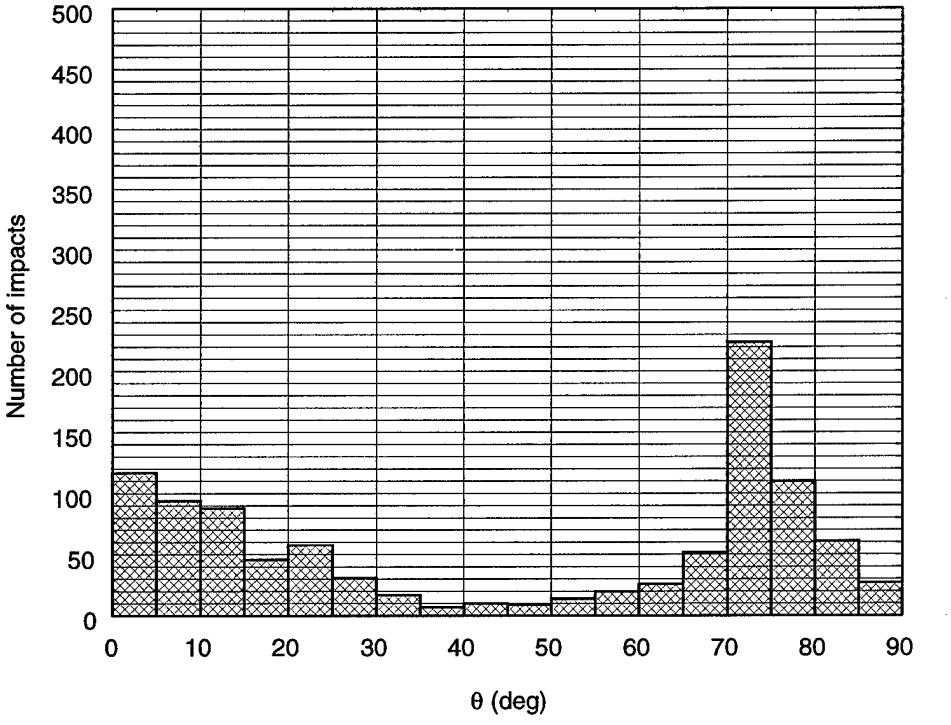

Figure 18: Impact angle histogram for 48 ft segment ($\sigma_{py} = 3$ deg/sec).

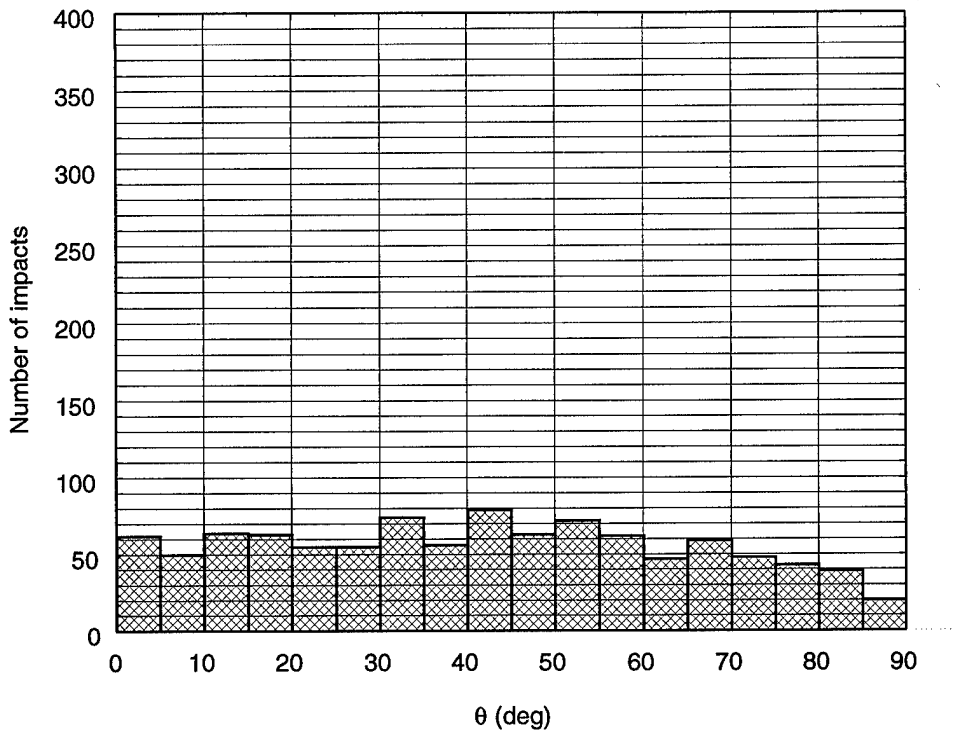

Figure 19: Impact angle histogram for 68 ft segment ($\sigma_{py} = 30$ deg/sec).

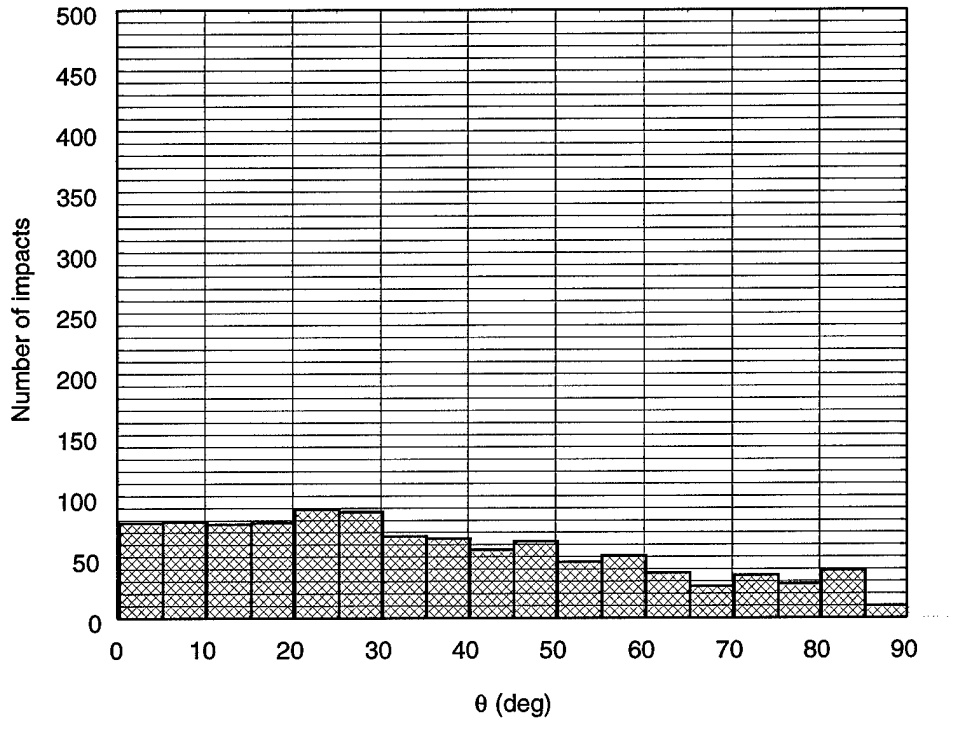

Figure 20: Impact angle histogram for 68 ft segment ($\sigma_{py} = 3$ deg/sec).

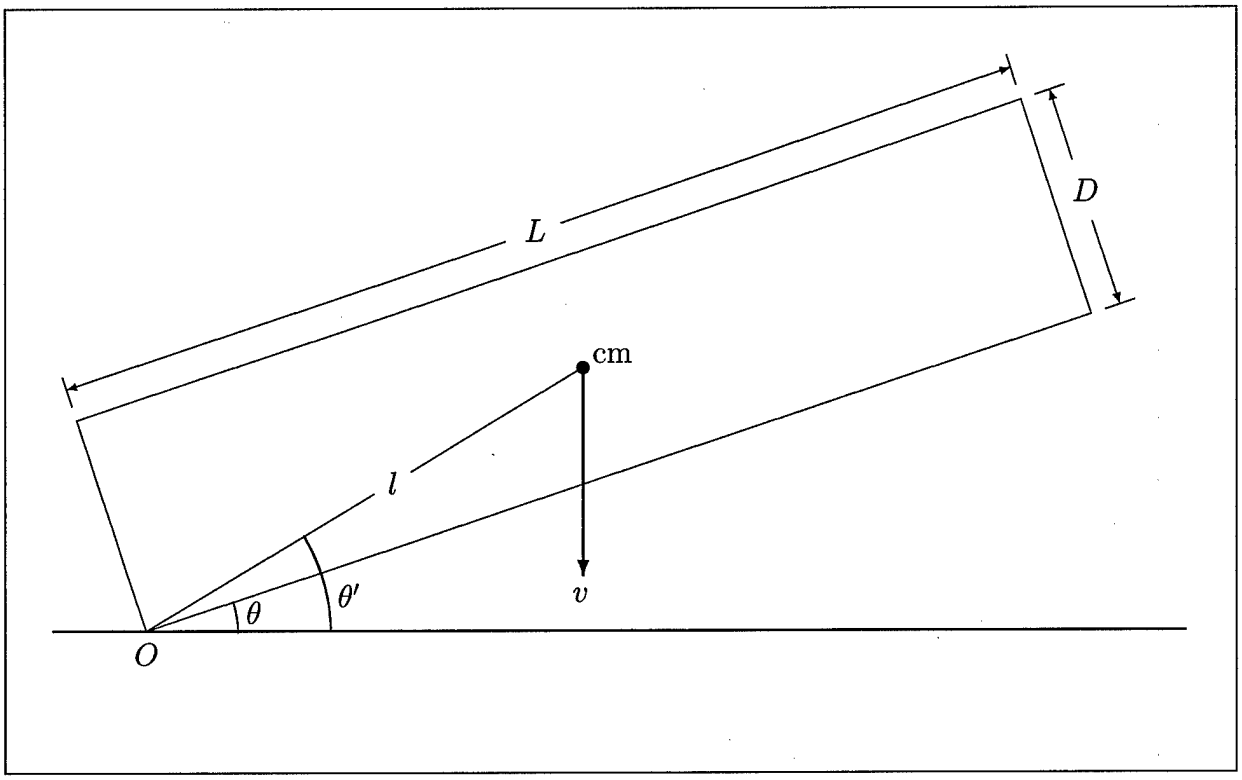

Figure 21: Impact orientation of cylinder.

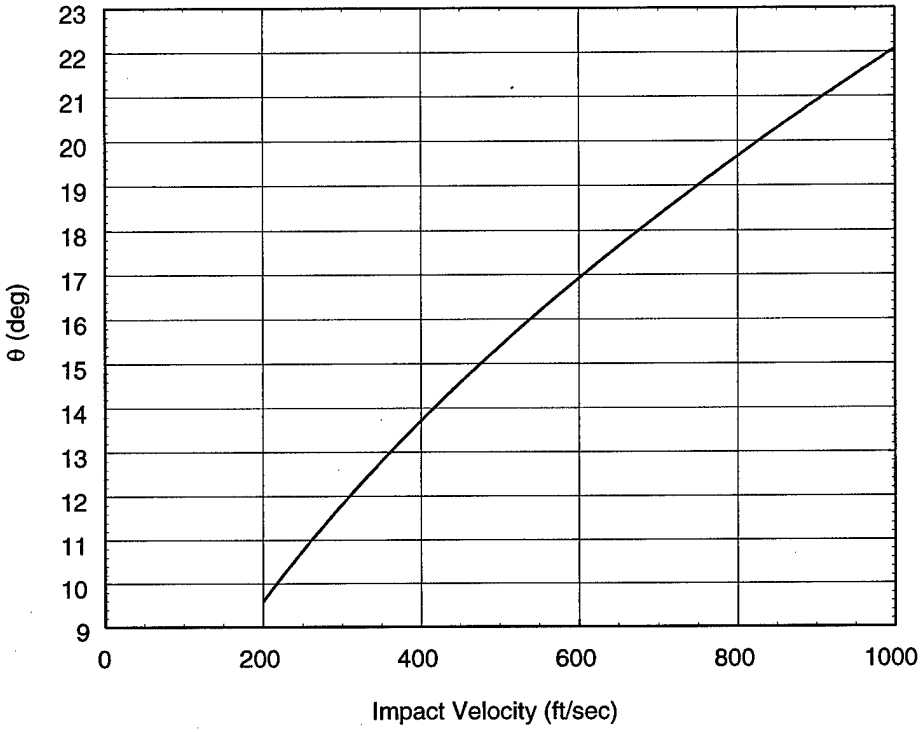

Figure 22: Maximum angle for side-on impact of 16 ft segment.

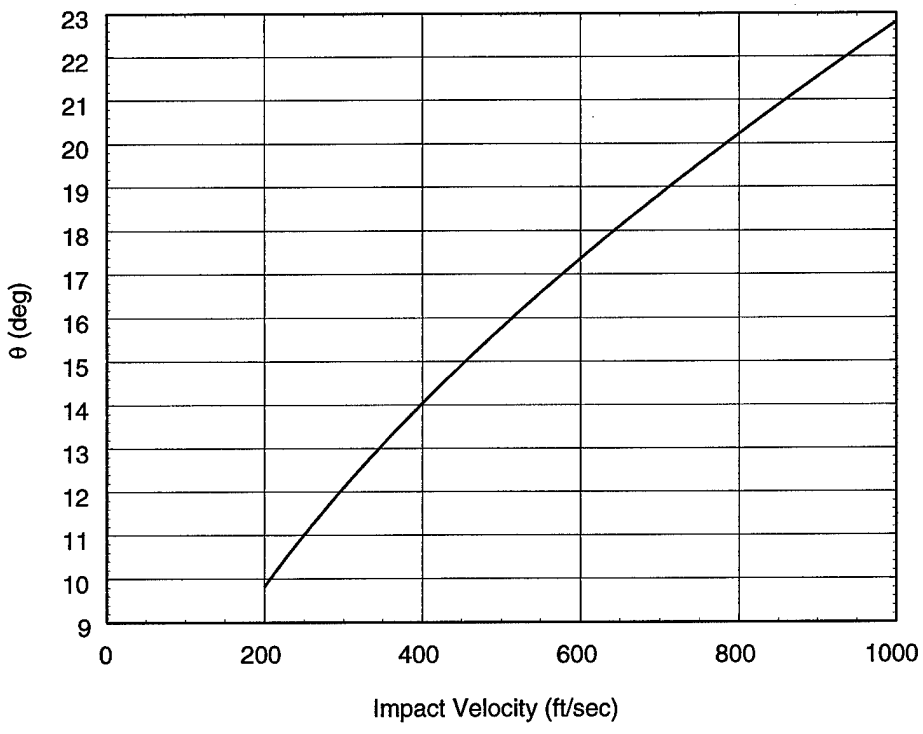

Figure 23: Maximum angle for side-on impact of 33 ft segment.

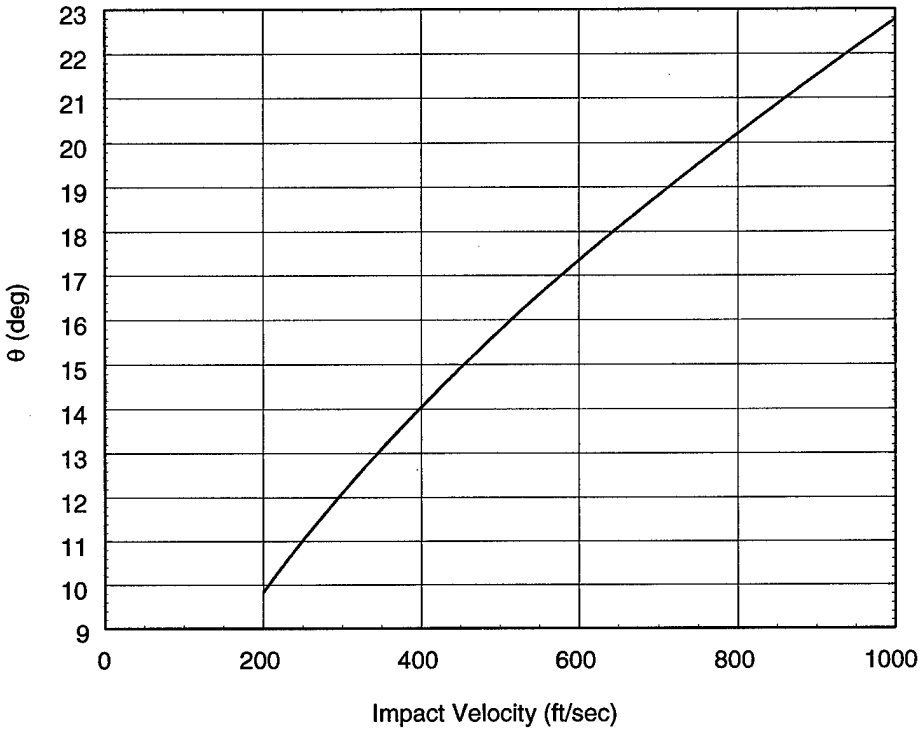

Figure 24: Maximum angle for side-on impact of 48 ft segment.

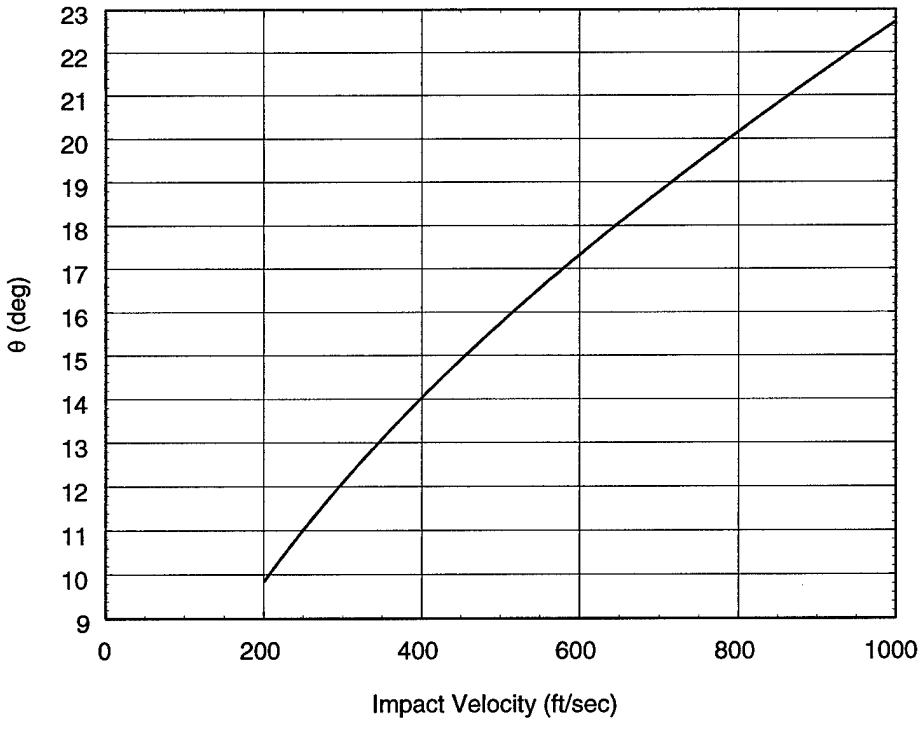

Figure 25: Maximum angle for side-on impact of 68 ft segment.